

# Detailed analysis of the chiral unitary model for meson-baryon scatterings with flavor SU(3) breaking effects

Tetsuo HYODO<sup>1</sup>, Seung-il NAM<sup>1,2</sup>, Daisuke JIDO<sup>1\*)</sup> and Atsushi HOSAKA<sup>1</sup>

<sup>1</sup>*Research Center for Nuclear Physics (RCNP), Ibaraki, Osaka 567-0047, Japan*

<sup>2</sup>*Department of Physics, Pusan National University, Pusan 609-735, Korea*

We study  $s$ -wave meson-baryon scatterings using the chiral unitary model. We consider  $1/2^-$  baryon resonances as quasibound states of the low lying mesons ( $\pi, K, \eta$ ) and baryons ( $N, \Lambda, \Sigma, \Xi$ ). In previous works, the subtraction constants which appeared in loop integrals largely depended on channels and it was necessary to fit these constants to reproduce the data. In order to extend this model to all channels with fewer parameters, we introduce flavor SU(3) breaking interactions in the framework of chiral perturbation theory. It is found, however, that the observed SU(3) breaking in meson-baryon scatterings cannot be explained by the present SU(3) breaking interactions. The essential physics of the resonances seems to lie in the subtraction constants.

## §1. Introduction

The study of meson-baryon scatterings of various channels in a unified way is important to understand hadron dynamics at low and intermediate energy regions from the viewpoint of QCD. Especially the properties of excited states of baryons observed in the meson-baryon scatterings as resonances are investigated with great interest both theoretically and experimentally. So far, there are several established approaches to describe the properties of the baryon resonances. A recent development in this field is the introduction of the chiral unitary model,<sup>1), 2), 3), 4), 5), 6)</sup> where the  $s$ -wave baryon resonances are dynamically generated in meson-baryon scatterings, while the conventional quark model approach describes the baryon resonances as three-quark states with an excitation of one of the quarks.

The chiral unitary model is based on the chiral perturbation theory (ChPT).<sup>7), 8)</sup> Imposing the unitarity condition, we can apply the ChPT at higher energy region than in the original perturbative calculation, and we can study properties of resonances generated by non-perturbative resummations. In the implementation of the unitarity condition, regularization of loop integrals brings parameters into this model, such as the three-momentum cut-off and the “subtraction constants” in the dimensional regularization.

In Refs. 1), 5), the  $s$ -wave scatterings of the meson and baryon systems with the strangeness  $S = -1$  were investigated by solving the Lippman-Schwinger equation in the coupled channels, where the  $\Lambda(1405)$  resonance was dynamically generated by the meson-baryon scatterings. In the regularization procedure, parameters were introduced for the finite ranges in the kernel potential,<sup>1)</sup> and for the three-momentum cut-off in the loop integral.<sup>5)</sup> In Refs. 9), 10), 11), they extended the chiral uni-

---

\*) Present address: ECT\*, European Centre for Theoretical Studies in Nuclear Physics and Related Areas Villa Tambosi, Strada delle Tabarelle 286, I-38050 Villazzano (Trento), Italy

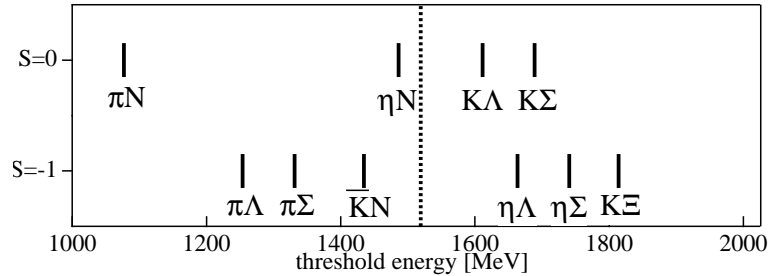


Fig. 1. Threshold energies of the meson-baryon scatterings in the  $S = -1$  and  $S = 0$  channels. The dotted line in the middle represents the averaged energy of all meson-baryon thresholds.

tary approach to other strangeness channels and obtained the baryonic resonances,  $\Lambda(1405)$ ,  $N(1535)$ ,  $\Lambda(1670)$ ,  $\Sigma(1620)$  and  $\Xi(1620)$ , as dynamically generated objects. They used the dimensional regularization scheme with channel dependent subtraction constants ( $a_i$ 's). In particular, the subtraction constants in  $S = 0$  depended significantly on channels, while as reported in Ref. 12), a common subtraction constant was found in the  $S = -1$  channel to reproduce the total cross sections of the  $K^-p$  scattering as well as  $\Lambda(1405)$  properties.

In this work, we raise a question whether such channel dependence of subtraction constants could be dictated by the flavor SU(3) breaking effects of an underlying theory, or not. As we will discuss in detail, it is shown that the subtraction constants should not be dependent on scattering channels in the SU(3) limit.<sup>14),15)</sup> The SU(3) breaking should have significant effects on observed quantities. This is expected from, for instance, the large dependence of the threshold energies on the meson-baryon channels as shown in Fig. 1. This is particularly the case for  $S = 0$ , where the lowest threshold energy of the  $\pi N$  channel deviates considerably from the mean value.

In order to study the above questions, we consider the following two cases;

- We use a common subtraction constant for all scattering channels and see whether this simplified calculation works or not.
- When this method does not work, we introduce the flavor SU(3) breaking effects in the interaction kernel.

In this way, we expect that the free parameters in the previous works could be controlled with suitable physics ground, which allows us to extend this method to other channels with predictive power. In this work, we concentrate on the  $s$  wave scatterings, since the  $p$  wave contribution to the total cross sections is shown to be small in the  $S = -1$  channel in Ref. 13).

This paper is a detailed study of the results in Ref. 15). In section 2, we present the formulation of the chiral unitary model. The calculation with a common subtraction constant and comparison with the previous works are shown in section 3. We then introduce the flavor SU(3) breaking effects in the interaction kernel and present numerical results in section 4. We discuss the results and summarize this work in section 5.

## §2. Formulation

In this section we review briefly the formulation of the chiral unitary model. We derive the basic interaction of meson-baryon scatterings from the lowest order chiral Lagrangian, and we maintain the unitarity of the S-matrix. There are several methods which recover the unitarity of the S-matrix such as solving the Bethe-Salpeter Equation (BSE),<sup>5)</sup> Inverse Amplitude Method (IAM),<sup>16)</sup> N/D method<sup>12)</sup> and so on. In this work, we adopt the N/D method,<sup>17)</sup> since this method provides a general form of the T-matrix using the dispersion relation and the analyticity of inverse of the T-matrix. Recently the N/D method has been applied to coupled channel meson-baryon scatterings.<sup>18),12)</sup> It was found that the final form of the T-matrix derived from the N/D method is essentially equivalent to the result of Ref. 5) derived from the BSE.

The chiral Lagrangian for baryons in the lowest order of the chiral expansion is given by<sup>19)</sup>

$$\mathcal{L}_{\text{lowest}} = \text{Tr} \left( \bar{B}(i\not{D} - M_0)B - D(\bar{B}\gamma^\mu\gamma_5\{A_\mu, B\}) - F(\bar{B}\gamma^\mu\gamma_5[A_\mu, B]) \right). \quad (2.1)$$

Here  $D$  and  $F$  are coupling constants. In Eq. (2.1) the covariant derivative  $\mathcal{D}_\mu$ , the vector current  $V_\mu$ , the axial vector current  $A_\mu$  and the chiral field  $\xi$  are defined by

$$\mathcal{D}_\mu B = \partial_\mu B + i[V_\mu, B], \quad (2.2)$$

$$V_\mu = -\frac{i}{2}(\xi^\dagger \partial_\mu \xi + \xi \partial_\mu \xi^\dagger), \quad (2.3)$$

$$A_\mu = -\frac{i}{2}(\xi^\dagger \partial_\mu \xi - \xi \partial_\mu \xi^\dagger), \quad (2.4)$$

$$\xi(\Phi) = \exp\{i\Phi/\sqrt{2}f\}, \quad (2.5)$$

where  $f$  is the meson decay constant, here we take an averaged value  $f = 1.15f_\pi$  with  $f_\pi = 93$  MeV. The meson and baryon fields are expressed in the SU(3) matrix form as

$$B = \begin{pmatrix} \frac{1}{\sqrt{2}}\Sigma^0 + \frac{1}{\sqrt{6}}\Lambda & \Sigma^+ & p \\ \Sigma^- & -\frac{1}{\sqrt{2}}\Sigma^0 + \frac{1}{\sqrt{6}}\Lambda & n \\ \Xi^- & \Xi^0 & -\frac{2}{\sqrt{6}}\Lambda \end{pmatrix}, \quad (2.6)$$

$$\Phi = \begin{pmatrix} \frac{1}{\sqrt{2}}\pi^0 + \frac{1}{\sqrt{6}}\eta & \pi^+ & K^+ \\ \pi^- & -\frac{1}{\sqrt{2}}\pi^0 + \frac{1}{\sqrt{6}}\eta & K^0 \\ K^- & \bar{K}^0 & -\frac{2}{\sqrt{6}}\eta \end{pmatrix}. \quad (2.7)$$

In the Lagrangian (2.1),  $M_0$  denotes a common mass of the octet baryons. However, we use the observed values of the baryon masses in the following calculations. The mass splitting among the octet baryons in the Lagrangian level will be introduced consistently with the SU(3) breaking in section 4.

The  $s$  wave interactions at the tree level come from the Weinberg-Tomozawa

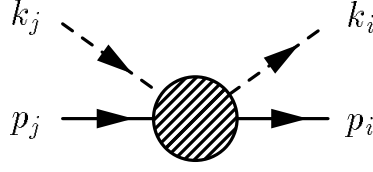


Fig. 2. Definition of the momentum variables. Dashed and solid lines represent mesons and baryons, respectively.

(WT) interaction, which is in the vector coupling term in the covariant derivative;

$$\mathcal{L}_{WT} = \text{Tr} \left( \bar{B} i \gamma^\mu \frac{1}{4f^2} [(\Phi \partial_\mu \Phi - \partial_\mu \Phi \Phi), B] \right). \quad (2.8)$$

From this Lagrangian, the meson-baryon scattering amplitude at the tree level is given by

$$\begin{aligned} V_{ij}^{(WT)} &= -\frac{C_{ij}}{4f^2} \bar{u}(p_i)(k_i + k_j)u(p_j) \\ &= -\frac{C_{ij}}{4f^2} (2\sqrt{s} - M_i - M_j) \sqrt{\frac{E_i + M_i}{2M_i}} \sqrt{\frac{E_j + M_j}{2M_j}}, \end{aligned} \quad (2.9)$$

where the indices  $(i, j)$  denote the channels of the meson-baryon scatterings and  $M_i$  and  $E_i$  are the observed mass and the energy of the baryon in the channel  $i$ , respectively. The channels  $(i, j)$  are shown in Table III in Appendix. The kinematics of this vertex is shown in Fig. 2 and  $s$  in Eq. (2.9) is defined as  $s = (k + p)^2$ . The last line is obtained in the center of mass frame with the nonrelativistic reduction. The coefficient  $C_{ij}$  is fixed by chiral symmetry and the explicit form of  $C_{ij}$  is shown in Ref. 5) for  $S = -1$  and in Ref. 10) for  $S = 0$ .

In the coupled channel formulation the T-matrix takes a matrix form. The unitarity condition is guaranteed by the optical theorem  $-2\text{Im}[T_{ii}] = T_{ik}\rho_k T_{ki}^*$ , which can be written as

$$2\text{Im}[T_{ii}^{-1}] = \rho_i, \quad (2.10)$$

where the normalization of the  $T$ -matrix is defined by

$$S_{ij} = 1 - i \left( \frac{\sqrt{2M_i|\mathbf{q}_i|2M_j|\mathbf{q}_j|}}{4\pi\sqrt{s}} \right) T_{ij}$$

With the condition (2.10) and the dispersion relation for  $T_{ii}^{-1}$ , we find a general form of the T-matrix using the N/D method. Following Ref. 12), we write

$$T_{ij}^{-1}(\sqrt{s}) = \delta_{ij} \left( \tilde{a}_i(s_0) + \frac{s - s_0}{2\pi} \int_{s_i^+}^{\infty} ds' \frac{\rho_i(s')}{(s' - s)(s' - s_0)} \right) + \mathcal{T}_{ij}^{-1}, \quad (2.11)$$

where  $s_i^+$  is the value of  $s$  at the threshold of the channel  $i$ , and  $s_0$  is the subtraction point. The parameter  $\tilde{a}_i(s_0)$  is the subtraction constant and is a free parameter

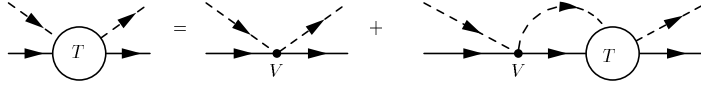


Fig. 3. Diagrammatic interpretation of Eq. (2.18).

within the N/D method. The matrix  $\mathcal{T}_{ij}$  is determined by the chiral perturbation theory as discussed later. In the derivation of Eq. (2.11), we have neglected the left hand cuts, which correspond to  $u$ -channel diagrams of the crossing symmetry.

Let us assume that the intermediate states of the meson-baryon scatterings are composed by one octet meson and one octet baryon. We do not consider multi-mesons and excited baryons, such as  $\pi\pi N$  and  $\pi\Delta$ . In this case, the phase space  $\rho_i$  in Eq. (2.10) is written as

$$\rho_i(\sqrt{s}) = \frac{2M_i|\mathbf{q}_i|}{4\pi\sqrt{s}}, \quad (2.12)$$

where  $\mathbf{q}_i$  is a three-momentum of the intermediate meson on the mass shell. Let us define the  $G$  function by

$$G_i(\sqrt{s}) = -\tilde{a}_i(s_0) - \frac{s-s_0}{2\pi} \int_{s_i^+}^{\infty} ds' \frac{\rho_i(s')}{(s'-s)(s'-s_0)}, \quad (2.13)$$

which takes the same form as, up to a constant, the ordinary meson-baryon loop function:

$$G_i(\sqrt{s}) = i \int \frac{d^4q}{(2\pi)^4} \frac{2M_i}{(P-q)^2 - M_i^2 + i\epsilon} \frac{1}{q^2 - m_i^2 + i\epsilon}. \quad (2.14)$$

This integral should be regularized by an appropriate regularization scheme. In the dimensional regularization, the integral is calculated as

$$\begin{aligned} G_i(\sqrt{s}) = \frac{2M_i}{(4\pi)^2} & \left\{ a_i(\mu) + \ln \frac{M_i^2}{\mu^2} + \frac{m_i^2 - M_i^2 + s}{2s} \ln \frac{m_i^2}{M_i^2} \right. \\ & + \frac{\bar{q}_i}{\sqrt{s}} \left[ \ln(s - (M_i^2 - m_i^2) + 2\sqrt{s}\bar{q}_i) + \ln(s + (M_i^2 - m_i^2) + 2\sqrt{s}\bar{q}_i) \right. \\ & \left. \left. - \ln(-s + (M_i^2 - m_i^2) + 2\sqrt{s}\bar{q}_i) - \ln(-s - (M_i^2 - m_i^2) + 2\sqrt{s}\bar{q}_i) \right] \right\}, \end{aligned} \quad (2.15)$$

where  $\mu$  is the regularization scale,  $a_i$  is the subtraction constant and  $\bar{q}_i$  is defined by

$$\bar{q}_i(\sqrt{s}) = \frac{\sqrt{(s - (M_i - m_i)^2)(s - (M_i + m_i)^2)}}{2\sqrt{s}}. \quad (2.16)$$

In the tree approximation, only the  $\mathcal{T}_{ij}$  term survives in Eq. (2.11), which may be identified with the WT interaction  $V^{(WT)}$  in Eq. (2.9). Therefore, the resulting

channel dependent $a_i$ ( $S = -1$ )						
channel	$\bar{K}N$	$\pi\Sigma$	$\pi\Lambda$	$\eta\Lambda$	$\eta\Sigma$	$K\Xi$
$a_i$	-1.84	-2.00	-1.83	-2.25	-2.38	-2.67

channel dependent $a_i$ ( $S = 0$ )				
channel	$\pi N$	$\eta N$	$K\Lambda$	$K\Sigma$
$a_i$	0.711	-1.09	0.311	-4.09

Table I. Channel dependent subtraction constants  $a_i$  used in Refs. 9), 10) with the regularization scale  $\mu = 630$  MeV. For the  $S = 0$  channel, although the original values of  $a_i$  are obtained with  $\mu = 1200$  MeV, here we show the values of  $a_i$  corresponding to  $\mu = 630$  MeV by using the relation  $a(\mu') = a(\mu) + 2 \ln(\mu'/\mu)$ .

T-matrix is written as

$$T^{-1} = -G + (V^{(WT)})^{-1} , \quad (2.17)$$

$$T = V^{(WT)} + V^{(WT)}GT . \quad (2.18)$$

This is the algebraic equation for the T-matrix, which corresponds to the integral BSE. The diagrammatic interpretation of Eq. (2.18) is shown in Fig. 3.

The subtraction constants  $a_i(\mu)$  in Eq. (2.15), in principle, would be related to the counter terms in the higher order Lagrangian in the chiral perturbation theory. In the previous works,<sup>9),10)</sup> they have fitted these subtraction constants( $a_i$ ) by using the data of  $\bar{K}N(S = -1)$  and  $\pi N(S = 0)$  scatterings. In Table I we show the subtraction constants used in Refs. 9), 10). In the table, in order to compare the channel dependence of the subtraction constants, we take the regularization scale at  $\mu = 630$  MeV in the both channels. Changing the regularization scale, the subtraction constants are simply shifted by  $a(\mu') = a(\mu) + 2 \ln(\mu'/\mu)$ . From this table we see that the  $a_i$  values in  $S = 0$  are very much different from each other. In the rest of this paper we refer to these parameters as “channel dependent  $a_i$ ”.

### §3. Calculation with a common subtraction constant

In this section, we show calculations in which a single subtraction constant  $a$  is commonly used in the meson-baryon loop function (2.15), in order to see the role of the channel dependent  $a_i$  to reproduce the observed cross sections and the resonance properties.

Let us first show that in the SU(3) limit together with the constraint in the chiral unitary model, there is only one subtraction constant.<sup>14),15)</sup> Under SU(3) symmetry, scattering amplitudes of one octet meson and one octet baryon are composed of SU(3) irreducible representations. The amplitudes satisfy the scattering equation in each representation,

$$T(D) = V(D) + V(D)G(D)T(D) , \quad (3.1)$$

where  $D$  represents an SU(3) irreducible representation,  $D = 1, 8, 8, 10, \bar{10}$  and 27. Therefore, on one hand, the functions  $G$ , or equivalently the subtraction constants  $a_i$  are represented by diagonal matrices in the SU(3) basis. On the other hand,

since  $G$  functions are given as a loop integrals as shown in (14) and (15), they are also diagonal in the particle basis  $(\pi^- p, \eta \Lambda, \dots)$ . These observations imply that the subtraction constants are components of a diagonal matrix both in SU(3) and particle bases, which are transformed uniquely by a unitary matrix of SU(3) Clebsch-Gordan coefficients;

$$a(D) = \sum_k U_{Dk} a_k (U^\dagger)_{kD} . \quad (3.2)$$

This can be happen when the subtraction constants is proportional to unity. Hence, subtraction constants are not dependent on channels in the SU(3) limit.

Now, we discuss the case of  $S = -1$ , where the subtraction constants  $a_i$  are not very dependent on the channels as shown in Table I. Therefore, it is expected that the calculation with a common  $a$  gives a good description by choosing a suitable value.

Next we study the  $S = 0$  channel using a common subtraction constant. Here we will find that the common  $a$  cannot reproduce simultaneously the resonance properties and the  $S_{11}$  amplitude at low energy region.

In order to concentrate on the role of the subtraction constants and to see the channel dependence, we assume the following simplifications for the calculations of the  $S = -1$  and  $S = 0$  channels;

- We use an averaged value for the meson decay constants,  $f = 1.15f_\pi = 106.95$  MeV, while in Ref. 10) physical values were taken as  $f_\pi = 93$  MeV,  $f_K = 1.22f_\pi$ ,  $f_\eta = 1.3f_\pi$ .
- We do not include the effect of vector meson exchanges and  $\pi\pi N$  channels to reproduce the  $\Delta(1620)$  resonance, which were considered in Ref. 10).

With these simplifications, the calculations in the  $S = -1$  and  $S = 0$  channels are based on exactly the same formulation; the differences are in the flavor SU(3) coefficients  $C_{ij}$  in Eq. (2.9) and in the channel dependent subtraction constants.

### 3.1. The $S = -1$ channel ( $\bar{K}N$ scattering)

In the  $S = -1$  channel, the subtraction constants  $a_i$  obtained in Ref. 9) are not very much dependent on the channels, as shown in Table I. In Ref. 12), they used a common  $a \sim -2$ , which was “naturally” obtained from the matching with the three-momentum cut-off regularization with  $\Lambda = 630$  MeV. In the both works, they reproduced very well the total cross sections of the  $K^- p$  scatterings and the mass distribution of the  $\pi\Sigma$  channel with  $I = 0$ , where the  $\Lambda(1405)$  resonance is seen. In Ref. 9), the  $\Lambda(1670)$  resonance was also obtained with the channel dependent subtraction constants, and its property was discussed by analyzing the speed plots in the  $I = 0$  channels.

Here we search one common  $a$  to be used in all channels in  $S = -1$ . In order to fix the common  $a$ , we use threshold properties of the  $\bar{K}N$  scatterings, which are

well observed in the branching ratios:<sup>20),21)</sup>

$$\begin{aligned}\gamma &= \frac{\Gamma(K^-p \rightarrow \pi^+\Sigma^-)}{\Gamma(K^-p \rightarrow \pi^-\Sigma^+)} \sim 2.36 \pm 0.04, \\ R_c &= \frac{\Gamma(K^-p \rightarrow \text{charged particles})}{\Gamma(K^-p \rightarrow \text{all})} \sim 0.664 \pm 0.011, \\ R_n &= \frac{\Gamma(K^-p \rightarrow \pi^0\Lambda)}{\Gamma(K^-p \rightarrow \text{neutral particles})} \sim 0.189 \pm 0.015.\end{aligned}\tag{3.3}$$

After fitting, we find the optimal value  $a = -1.96$ , with which the threshold branching ratios are obtained as shown in Table II. The result using the common  $a = -1.96$  does not differ very much from that of channel dependent ones, and also the value  $a = -1.96$  is close to an averaged value of the channel dependent subtraction constants  $a_i$ , namely  $\sim -2.15$ . Therefore, the threshold properties are not sensitive to such a fine tuning of the subtraction constants.

Using the common  $a = -1.96$ , we calculate the total cross sections of the  $K^-p$  scatterings (Fig. 4, solid lines), the T-matrix amplitude of the  $\bar{K}N$  scattering with  $I = 0$  (Fig. 5, solid lines) and the mass distributions of the  $\pi\Sigma$  channel with  $I = 0$  (Fig. 6, solid lines). We also plot the calculations with the channel dependent  $a_i$  obtained in Ref. 9) in Figs. 4,5 and 6 as the dotted lines. Here we find that the present calculations are slightly different from the calculations with the channel dependent  $a_i$  in the total cross sections and the  $\pi\Sigma$  mass distributions. Therefore, the  $\Lambda(1405)$  resonance is well reproduced with the common  $a = -1.96$ , which is consistent with the results in Ref. 12). However, the resonance  $\Lambda(1670)$  disappears when the common  $a$  is used, as we see in the T-matrix amplitude of  $\bar{K}N \rightarrow \bar{K}N$  with  $I = 0$  in Fig. 5. As pointed out in Ref. 9), the  $\Lambda(1670)$  resonance structure is very sensitive to the value of  $a_{K\Xi}$ . Indeed we have checked that the  $\Lambda(1670)$  resonance is reproduced when we choose  $a_{K\Xi} \sim -2.6$  with the other  $a_i$  unchanged,  $-1.96$ .

If we choose  $a = -2.6$  for all subtraction constants, the threshold branching ratios are calculated as  $\gamma = 2.41$ ,  $R_c = 0.596$  and  $R_n = 0.759$ , and the agreement with the experimental data becomes poor, as shown in Figs. 4 and 5. In particular, the  $K^-p \rightarrow \bar{K}^0n$  cross section is underestimated, and also the resonance structure of  $\Lambda(1405)$  disappears in the  $\pi\Sigma$  mass distribution (Fig. 6). As we change all subtraction constants from  $a = -1.96$  to  $a = -2.6$  gradually, the position of the peak of  $\Lambda(1405)$  moves to lower energy side and finally disappears under the  $\pi\Sigma$  threshold. Therefore, taking common  $a \sim -2$  is essential to reproduce the resonance properties of  $\Lambda(1405)$  and the total cross sections of the  $K^-p$  scatterings in the low energy region.

### 3.2. The $S = 0$ channel ( $\pi N$ scattering)

In Ref. 10), the total cross sections of the  $\pi^-p$  inelastic scatterings and the resonance properties of the  $N(1535)$  were reproduced well by using the channel dependent  $a_i$ . After the simplification for  $f$  and inelastic channels, the agreement with the data is still acceptable, as shown in Figs. 7 and 8 by dotted lines, as long as the channel dependent  $a_i$  are employed. In the T-matrix elements of the  $\pi N$



	$\gamma$	$R_c$	$R_n$
experiment	$2.36 \pm 0.04$	$0.664 \pm 0.011$	$0.189 \pm 0.015$
channel dep. $a_i$	1.73	0.629	0.195
common $a$	1.80	0.624	0.225
SU(3) breaking	2.19	0.623	0.179

Table II. Threshold branching ratios calculated with the channel dependent  $a_i$ , the common  $a = -1.96$ , and  $a = -1.59$  with the SU(3) breaking interaction. The experimental values are taken from Refs. 20), 21).

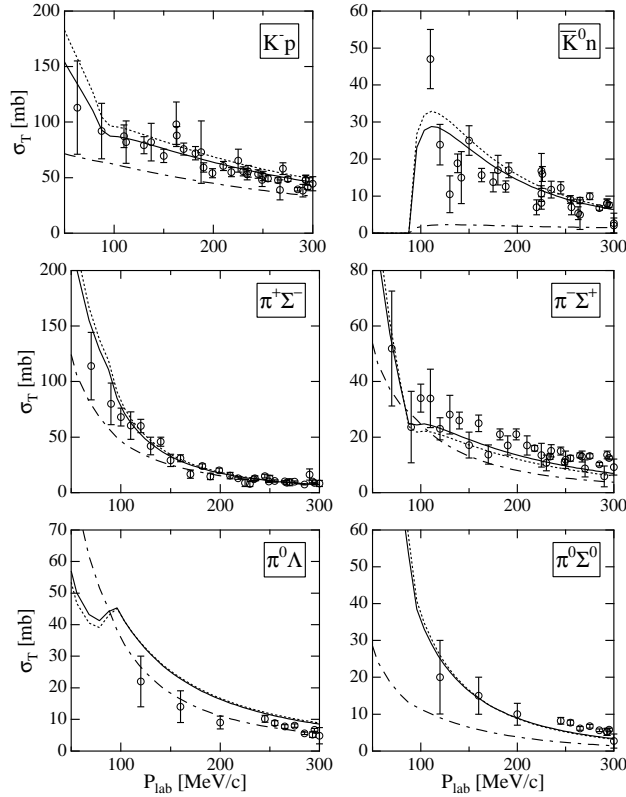


Fig. 4. Total cross sections of  $K^-p$  scatterings ( $S = -1$ ) as functions of  $P_{\text{lab}}$ , the three-momentum of initial  $K^-$  in the laboratory frame. Dotted lines show the results with the channel dependent  $a_i$ , solid lines show the results with the common  $a = -1.96$ , and dash-dotted lines show the results with the common  $a = -2.6$ . Open circles with error bars are experimental data taken from Refs. 22), 23), 24), 25), 26), 27), 33), 28), 29), 30), 31), 32).

scattering in the  $S_{11}$  channel, we see a kink structure around the energy  $\sqrt{s} \sim 1500$  MeV, which corresponds to the  $N(1535)$  resonance.<sup>10)</sup>

In the previous subsection, we obtained the common subtraction constant  $a = -1.96$  with which the  $\bar{K}N$  total cross sections and the  $\Lambda(1405)$  properties are reproduced well. First, we use this common  $a$  for the  $S = 0$  channel. Shown in Figs. 7 and 8 by dash-dotted lines are the results with  $a = -1.96$  for the total cross sections

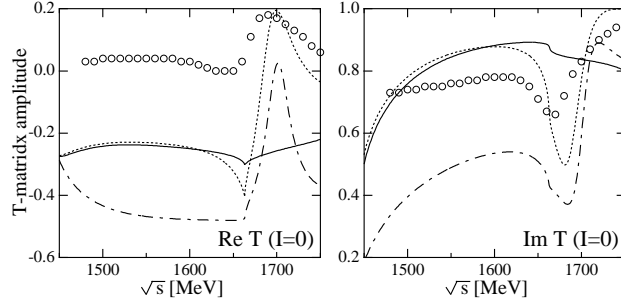


Fig. 5. Real and imaginary parts of the T-matrix amplitude of  $\bar{K}N \rightarrow \bar{K}N$  with  $I = 0$ . Dotted lines show the results with the channel dependent  $a_i$ , solid lines show the results with the common  $a = -1.96$ , and dash-dotted lines show the results with the common  $a = -2.6$ . Open circles are experimental data taken from Ref. 34).

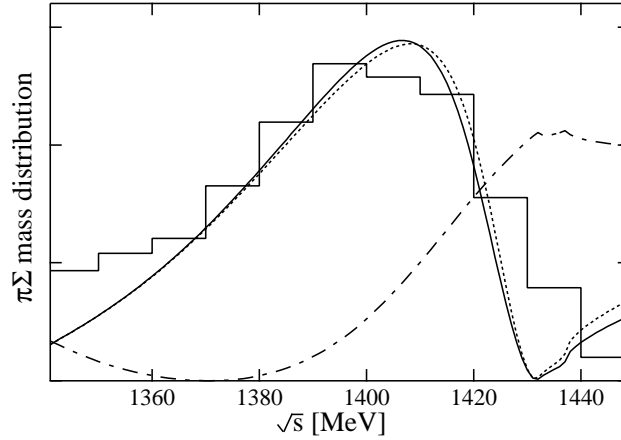


Fig. 6. The mass distributions of the  $\pi\Sigma$  channel with  $I = 0$ . Dotted line shows the result with the channel dependent  $a_i$ , solid line shows the result with the common  $a = -1.96$ , and dash-dotted line shows the result with the common  $a = -2.6$ . Histogram is experimental data taken from Ref. 35).

of the  $\pi^-p \rightarrow \pi^0\eta$ ,  $K^0\Lambda$  and  $K^0\Sigma$  scatterings, and the  $S_{11}$  T-matrix amplitude of  $\pi N \rightarrow \pi N$ . As can be seen in Figs. 7 and 8, the results with  $a = -1.96$  in the  $S = 0$  channel are far from the experimental data. In particular, in the  $\pi^-p \rightarrow \eta n$  cross section, the threshold behavior disagrees with the experiment, and the resonance structure of  $N(1535)$  disappears. In addition, as shown in Fig. 8, the T-matrix amplitude of the  $S_{11}$  channel is overestimated and an unexpected resonance has been generated at around  $\sqrt{s} \sim 1250$  MeV.

Next we search the single optimal subtraction constant within the  $S = 0$  channel, since the unnecessary resonance are obtained with  $a = -1.96$  at low energy. In order to avoid the appearance of such an unphysical resonance, we determine the common subtraction constant  $a$  so as to reproduce observed data up to  $\sqrt{s} = 1400$  MeV. The optimal value is found to be  $a = 0.53$ . The calculated  $S_{11}$  amplitude

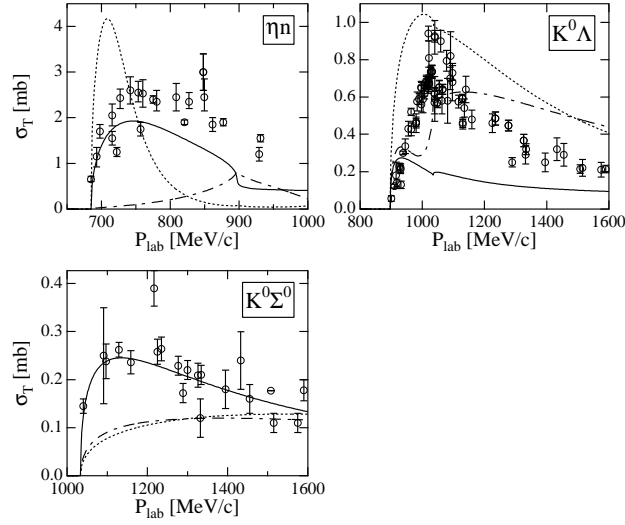


Fig. 7. Total cross sections of  $\pi^- p$  scatterings ( $S = 0$ ) as functions of  $P_{\text{lab}}$ , the three-momentum of initial  $\pi^-$  in the laboratory frame. Dotted lines show the results with channel dependent  $a_i$ , dash-dotted lines show the results with the common  $a = -1.96$ , obtained in  $S = -1$ , and solid lines show the results with the common  $a = 0.53$ . Open circles with error bars are experimental data taken from Refs. 36), 37), 38), 39), 40), 41), 42), 43), 44), 45), 46), 47), 48), 49), 50), 51), 52), 53), 54), 55).

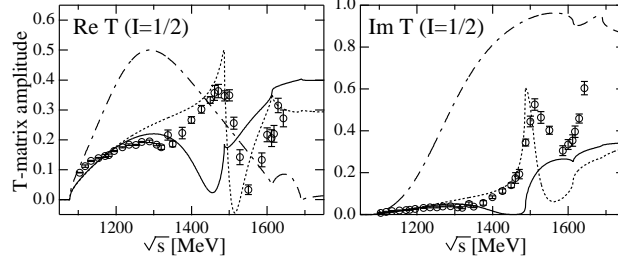


Fig. 8. Real and imaginary parts of the  $S_{11}$  T-matrix amplitudes of  $\pi N \rightarrow \pi N$ . Dotted lines show the results with channel dependent  $a_i$ , dash-dotted lines show the results with the common  $a = -1.96$ , obtained in  $S = -1$ , and solid lines show the results with the common  $a = 0.53$ . Open circles with error bars are experimental data taken from Ref. 56).

as well as the total cross sections are plotted in Figs. 7 and 8 by the solid lines. With this subtraction constant, the low energy behavior of the  $S_{11}$  amplitude of  $\pi N$  scatterings ( $\sqrt{s} < 1400$  MeV) is well reproduced, while, however, the  $N(1535)$  resonance structure is not still generated. We have also checked that there is no pole in the scattering amplitudes in the second Riemann sheet. Therefore, we conclude that in the  $S = 0$  channel we cannot reproduce simultaneously the  $N(1535)$  resonance and the  $S_{11}$  amplitude at low energy if a single subtraction constant is used.

#### §4. Flavor SU(3) breaking interactions

In the previous studies, it has been found that the channel dependent subtraction constants  $a_i$  are crucial in order to reproduce important features of experimental data. In this section, we consider SU(3) breaking terms of the chiral Lagrangian in order to see if the channel dependence in the subtraction constants can be absorbed into those terms. In this way, we are hoping that the number of free parameters could be reduced and that the origin of the channel dependence would be clarified.

##### 4.1. Flavor SU(3) breaking terms in the chiral Lagrangian

Here we introduce the flavor SU(3) breaking effects in the chiral Lagrangian by the quark masses. They are obtained by assuming that the current quark mass matrix  $\mathbf{m}$  is transformed under the chiral transformation as  $\mathbf{m} \rightarrow R\mathbf{m}L^\dagger$  and  $\mathbf{m}^\dagger = \mathbf{m}$ . Here we maintain isospin symmetry, namely  $\mathbf{m} = \text{diag}(\hat{m}, \hat{m}, m_s)$ . Then the SU(3) breaking terms are given uniquely up to order  $\mathcal{O}(m_q)$  as<sup>19)</sup>

$$\begin{aligned} \mathcal{L}_{SB} = & -\frac{Z_0}{2}\text{Tr}\left(d_m\bar{B}\{\xi\mathbf{m}\xi + \xi^\dagger\mathbf{m}\xi^\dagger, B\} + f_m\bar{B}[\xi\mathbf{m}\xi + \xi^\dagger\mathbf{m}\xi^\dagger, B]\right) \\ & -\frac{Z_1}{2}\text{Tr}(\bar{B}B)\text{Tr}(\mathbf{m}U + U^\dagger\mathbf{m}) , \end{aligned} \quad (4.1)$$

where  $f_m + d_m = 1$  and  $U(\Phi) = \xi^2 = \exp\{i\sqrt{2}\Phi/f\}$ . In this Lagrangian, there are three free parameters,  $Z_0, Z_1, f_m/d_m$ , which are determined by the baryon masses and the  $\pi N$  sigma term. Here we take  $m_s/\hat{m} = 26$ , which are determined in ChPT from the meson masses. According to the chiral counting rule, these quark mass terms are regarded as quantities of order  $\mathcal{O}(p^2)$ , if we assume the Gell-Mann-Oakes-Renner relation,<sup>57)</sup> which tells  $m_q \propto m_\pi^2$ . In this work, since we concentrate on the SU(3) breaking effect, we take into account only the terms of Eq. (4.1), and other terms of order  $\mathcal{O}(p^2)$  are not included.

Expanding the Lagrangian (4.1) in powers of the meson fields, the zeroth order terms contribute to the baryon mass splitting, which automatically satisfy the Gell-Mann-Okubo (GMO) mass formula.<sup>58), 59)</sup> From the mass splitting among the octet baryons and the  $\pi N$  sigma term, which we take here  $\sigma_{\pi N} = 36.4$  MeV, the parameters in the Lagrangian (4.1) are determined as

$$Z_0 = 0.528 , \quad Z_1 = 1.56 , \quad f_m/d_m = -0.31 , \quad (4.2)$$

and  $M_0 = 759$  MeV in the Lagrangian (2.1).

The meson-baryon interaction Lagrangian with the SU(3) breaking is obtained by picking up the terms with two meson fields. We find

$$\begin{aligned} \mathcal{L}_{SB}^{(2)} = & \frac{Z_0}{4f^2}\text{Tr}\left(d_m\bar{B}\{(2\Phi\mathbf{m}\Phi + \Phi^2\mathbf{m} + \mathbf{m}\Phi^2), B\} + f_m\bar{B}[(2\Phi\mathbf{m}\Phi + \Phi^2\mathbf{m} + \mathbf{m}\Phi^2), B]\right) \\ & + \frac{Z_1}{f^2}\text{Tr}(\bar{B}B)\text{Tr}(\mathbf{m}\Phi^2) . \end{aligned} \quad (4.3)$$

From this Lagrangian the basic interaction is given by

$$V_{ij}^{(SB)} = -\frac{1}{f^2} \left[ Z_0 \left( (A_{ij}^d d_m + A_{ij}^f f_m) \hat{m} + (B_{ij}^d d_m + B_{ij}^f f_m) m_s \right) + Z_1 \delta_{ij} B_i^e \right] \sqrt{\frac{E_i + M_i}{2M_i}} \sqrt{\frac{E_j + M_j}{2M_j}}. \quad (4.4)$$

The explicit forms of the coefficients  $A_{ij}$  and  $B_{ij}$  are given in Appendix. These interaction terms are independent of the meson momenta unlike the WT interaction (2.9).

Adding Eq. (4.4) to Eq. (2.9) and substituting them into Eq. (2.18), we obtain the unitarized T-matrix with the flavor SU(3) breaking effects as

$$T = \left[ 1 - \left( V^{(WT)} + V^{(SB)} \right) G \right]^{-1} \left( V^{(WT)} + V^{(SB)} \right). \quad (4.5)$$

Since we have already fitted the all parameters in the chiral Lagrangian, our parameters in the chiral unitary model with the SU(3) breaking effects are only the subtraction constants.

#### 4.2. The $S = -1$ channel

We follow the same procedures as in the calculations without the SU(3) breaking terms. First of all, we determine a common subtraction constant  $a$  from the threshold branching ratios (3.3). Then the optimal value is found to be  $a = -1.59$ . With this value, the total cross sections of the  $K^-p$  scatterings, the  $\pi\Sigma$  mass distribution and the scattering amplitude of  $\bar{K}N \rightarrow \bar{K}N$  with  $I = 0$  are plotted in Figs. 9, 10 and 11 by dash-dotted lines. As seen in the Fig. 9, for all the total cross sections, the inclusion of the SU(3) breaking terms with the common  $a$  makes the agreement with data worse, although the threshold branching ratios are produced much better than the previous works, as seen in Table II.

In the  $\pi\Sigma$  mass distribution shown in Fig. 11 (dash-dotted line), a sharp peak is seen, in obvious contradiction with the observed spectrum, which means that the important resonance structure of  $\Lambda(1405)$  has been lost. However, we find two poles of the T-matrix amplitude at  $z_1 = 1424 + 1.6i$  and  $z_2 = 1389 + 135i$  in the second Riemann sheet. It is reported that there are two poles in the T-matrix amplitude around the energy region of  $\Lambda(1405)$  in Refs. (60), (12), (61), (62). A detailed study of the two poles for  $\Lambda(1405)$  has been recently done in the viewpoint of the SU(3) flavor symmetry in Ref. (14). The inclusion of the SU(3) breaking terms does not change this conclusion, although the positions of the poles change.

We also calculate the total cross sections and the  $\pi\Sigma$  mass distribution with the physical values of the meson decay constants,  $f_\pi = 93$  MeV,  $f_K = 1.22f_\pi$ ,  $f_\eta = 1.3f_\pi$ . The calculated results are shown in Figs. 9, 10 and 11 by solid lines. The optimal value of the subtraction constants is  $a = -1.68$  to reproduce the threshold branching ratios as  $\gamma = 2.35$ ,  $R_c = 0.626$  and  $R_n = 0.172$ . The SU(3) breaking effect on the meson decay constants is not so large in the total cross sections, as seen in the figures. However, the shape of the peak seen in the  $\pi\Sigma$  mass distribution becomes wider than that in the calculation with the averaged meson decay constant.

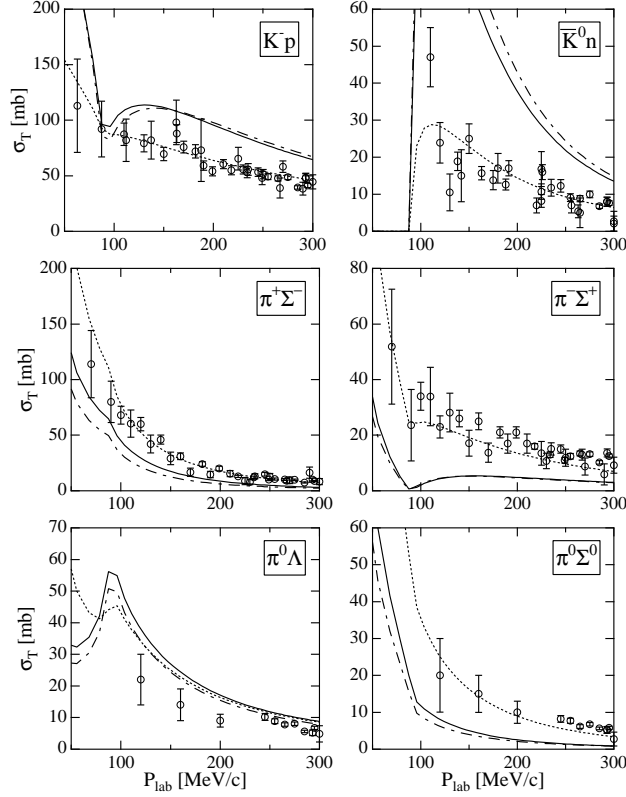


Fig. 9. Total cross sections of  $K^-p$  scatterings ( $S = -1$ ) as functions of  $P_{\text{lab}}$ , the three-momentum of initial  $K^-$  in the laboratory frame. Dotted lines show the results with the common  $a = -1.96$ , dash-dotted lines show the results including the SU(3) breaking with the common  $a = -1.59$ , and solid lines show the results including the SU(3) breaking and the physical  $f$  with the common  $a = -1.68$ . Open circles with error bars are experimental data taken from Refs. (22), (23), (24), (25), (26), (27), (28), (29), (33), (30), (31), (32).

Indeed we find again two poles in the scattering amplitudes at  $z'_1 = 1424 + 2.6i$  and  $z'_2 = 1363 + 87i$  in the second Riemann sheet. Compared with the poles  $z_1$  and  $z_2$  obtained in the above calculation, the position of the pole  $z'_2$  moves to lower energy side and approaches the real axis. The reason why the position of  $z'_2$  changes is understood as follows. Since  $z_2$  has large imaginary part, which means large width, and only the  $\pi\Sigma$  channel opens in this energy region, the resonance represented by the pole  $z_2$  has strong coupling to the  $\pi\Sigma$  channel. This fact implies that the position of the pole  $z_2$  is sensitive to the  $\pi\Sigma$  interaction. In the present calculation, the pion decay constant (93 MeV) is smaller than the averaged value (106.95 MeV) used in the above calculation, so that the attractive interaction of  $\pi\Sigma$  becomes stronger. It shifts the position of the pole  $z_2$  to lower energy side. Simultaneously, this suppresses the phase space of the decay of the resonance to the  $\pi\Sigma$  channel, and hence, the position of the pole approaches the real axis.

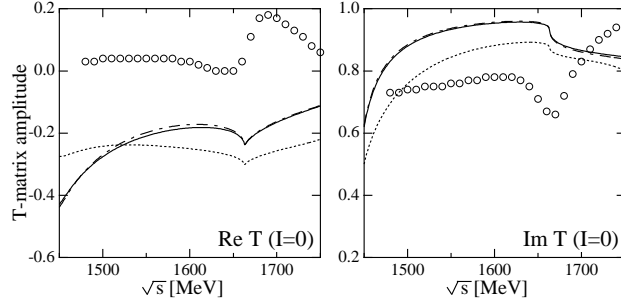


Fig. 10. Real and imaginary parts of the T-matrix amplitude of  $\bar{K}N \rightarrow \bar{K}N$  with  $I = 0$ . Dotted lines show the results with the common  $a = -1.96$ , dash-dotted lines show the results including the SU(3) breaking with the common  $a = -1.59$ , and solid lines show the results including the SU(3) breaking and the physical  $f$  with the common  $a = -1.68$ . Open circles are experimental data taken from Ref. 34).

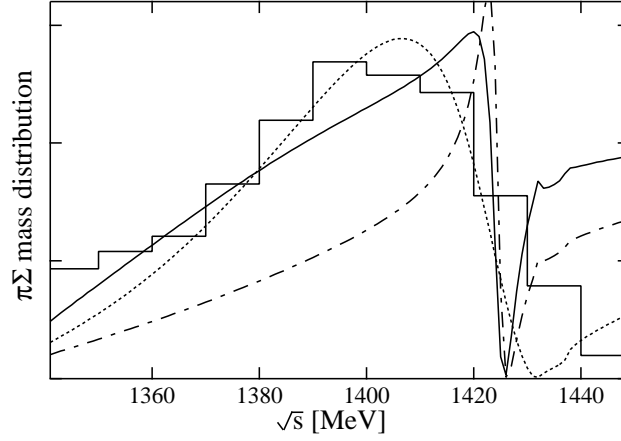


Fig. 11. Mass distributions of the  $\pi\Sigma$  channel with  $I = 0$ . Dotted line shows the result with the common  $a = -1.96$ , dash-dotted line shows the result including the SU(3) breaking with the common  $a = -1.59$ , and solid line shows the result including the SU(3) breaking and the physical  $f$  with the common  $a = -1.68$ . Histogram are experimental data taken from Ref. 35).

#### 4.3. The $S = 0$ channel

Here we show calculations in the  $S = 0$  channel with the SU(3) breaking terms. With a common  $a \sim -1.5$ , in which the threshold properties are reproduced well in the  $S = -1$  channel, we obtain still the large contribution in the  $S_{11}$   $\pi N$  scattering amplitude at the low energy as in the calculation without the SU(3) breaking effects. From this analysis, it is found that the low energy behavior of the  $\pi N$  scatterings cannot be reproduced as long as we use the common  $a \sim -2$ , even if we introduce the SU(3) breaking effects.

In order to search the optimal value of the common subtraction constant within the  $S = 0$  channel, we perform fitting of the T-matrix elements in the  $\pi N$   $S_{11}$  channel in low energy region up to 1400 MeV. We find  $a = 1.33$ . The results including the

SU(3) breaking effects with  $a = 1.33$  are shown as dash-dotted lines in Figs. 12 and 13. As seen in Fig. 13, the fitting is well performed up to  $\sqrt{s} \sim 1400$  MeV, while, however, the resonance structure does not appear around the energies of  $N(1535)$ .

Finally we show the calculations with the physical values of the meson decay constants in Figs. 12 and 13 (solid lines). The optimal value of the common subtraction constant is found to be  $a = 2.24$ . The results with the physical meson decay constants and  $a = 2.24$  are very similar to the calculation with the averaged value of the decay constants and  $a = 1.33$ . In this sense, the SU(3) breaking effect of the meson decay constant  $f$  is absorbed into the change of the common subtraction constant  $a$ .

In closing this section, we conclude that even if we introduce the SU(3) breaking effects in the Lagrangian level, the SU(3) breaking in the channel dependent subtraction constants  $a_i$  cannot be absorbed into the SU(3) breaking effects in the fundamental interactions in the both  $S = -1$  and  $S = 0$  channels.

## §5. Summary and discussions

In this work, first we have tried to use a single common subtraction constant in order to describe meson-baryon scatterings and baryon resonances in a unified way. In the  $S = -1$  channel,  $a \sim -2$  is fixed from the threshold branching ratios of the  $K^-p$  scatterings. With this parameter, the total cross sections of the  $K^-p$  scatterings are reproduced well, as well as the mass distribution for  $\Lambda(1405)$  is. However, in this case the  $\Lambda(1670)$  resonance cannot be reproduced. The subtraction constant  $a \sim -2$  corresponds to  $\Lambda = 630$  MeV in the three-momentum cut-off regularization of the meson-baryon loop integral.<sup>12)</sup> This value is consistent with the one often used in single nucleon processes.<sup>63)</sup> The elementary interaction of the  $\bar{K}N$  system is sufficiently attractive, and a resummation of the coupled channel interactions provides the  $\Lambda(1405)$  resonance at the correct position, by imposing the unitarity condition and by using the natural value for the cut-off parameter. Hence the wave function of  $\Lambda(1405)$  is largely dominated by the  $\bar{K}N$  component.

On the other hand, in the  $S = 0$  channel, if one uses the natural value for the subtraction constant as in the  $S = -1$  channel, the attraction of the meson-baryon interaction becomes so strong that an unexpected resonance is generated at around  $\sqrt{s} \sim 1250$  MeV. Therefore, repulsive component is necessary to reproduce the observed  $\pi N$  scattering. The fitted subtraction constant using the low energy  $\pi N$  scattering amplitude is  $a \sim 0.5$ . With this value, however, the  $N(1535)$  resonance is not generated, while the agreement in the cross sections of  $\pi^-p \rightarrow \eta n$  is rather good due to the threshold effects.

The unitarized amplitudes are very sensitive to the attractive component of the interaction. The interaction terms of the ChPT alone do not explain all scattering amplitudes simultaneously, but they must be complemented by the subtraction constants in the chiral unitary model. For small  $a$ , the interaction becomes more attractive, and for large  $a$ , less attractive. For  $S = 0$ , we need to choose  $a \sim 0.5$  in order to suppress the attraction from the  $\pi N$  interaction in contrast to the natural value  $a \sim -2$  in the  $S = -1$  channel. Therefore, it is not possible to reproduce both



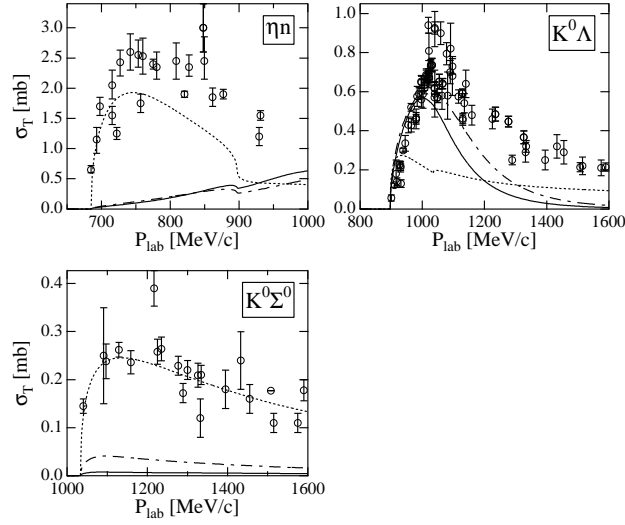


Fig. 12. Total cross sections of  $\pi^- p$  scatterings ( $S = 0$ ) as functions of  $P_{\text{lab}}$ , the three-momentum of initial  $\pi^-$  in the laboratory frame. Dotted lines show the results with the common  $a = 0.53$ , dash-dotted lines show the results including the SU(3) breaking interaction with the common  $a = 1.33$ , and solid lines show the results including the SU(3) breaking and the physical  $f$  with the common  $a = 2.24$ . Open circles with error bars are experimental data taken from Refs. 36), 37), 38), 39), 40), 41), 42), 43), 44), 45), 46), 47), 48), 49), 50), 51), 52), 53), 54), 55).

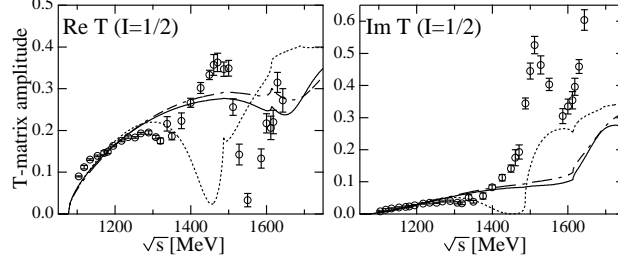


Fig. 13. Real and imaginary parts of the  $S_{11}$  T-matrix amplitudes of  $\pi N \rightarrow \pi N$ . Dotted lines show the results with the common  $a = 0.53$ , dash-dotted lines show the results including the SU(3) breaking interaction with the common  $a = 1.33$ , and solid lines show the results including the SU(3) breaking and the physical  $f$  with the common  $a = 2.24$ . Open circles with error bars are experimental data taken from Ref. 56).

the  $\Lambda(1405)$  resonance properties and the low energy  $\pi N$  scattering with a common subtraction constant.

Next we have introduced the flavor SU(3) breaking Lagrangian, with the hope that the channel dependence in the subtraction constants would be absorbed into the coefficients in the chiral Lagrangian. The coefficients can be determined from other observables, and hence they are more controllable than the subtraction constants which have to be fitted by the experimental data. However, the channel dependence of the subtraction constants in each strangeness channel cannot be replaced by the SU(3) breaking Lagrangian, although we have exhausted possible breaking sources up

Table III. Channels of meson-baryon scatterings. In this work we calculate the channels in ( $S = -1, Q = 0$ ) and ( $S = 0, Q = 0$ ).

$Y$	$S$	$I_3$	$Q$	channels
-2	-3	1	0	$K^0 \Xi^0$
		0	-1	$K^- \Xi^0, \bar{K}^0 \Xi^-$
		-1	-2	$K^- \Xi^-$
-1	-2	$\frac{3}{2}$	1	$\pi^+ \Xi^0, K^0 \Sigma^+$
		$\frac{1}{2}$	0	$\pi^0 \Xi^0, \pi^+ \Xi^-, \eta \Xi^0, \bar{K}^0 \Lambda, \bar{K}^0 \Sigma^0, K^- \Sigma^+$
		$-\frac{1}{2}$	-1	$\pi^0 \Xi^-, \pi^- \Xi^0, \eta \Xi^-, K^- \Lambda, K^- \Sigma^0, \bar{K}^0 \Sigma^-$
		$-\frac{3}{2}$	-2	$\pi^- \Xi^-, K^- \Sigma^-$
0	-1	2	2	$\pi^+ \Sigma^+$
		1	1	$\bar{K}^0 p, \pi^0 \Sigma^+, \pi^+ \Sigma^0, \pi^+ \Lambda, \eta \Sigma^+, K^+ \Xi^0$
		0	0	$K^- p, \bar{K}^0 n, \pi^0 \Lambda, \pi^0 \Sigma^0, \eta \Lambda, \eta \Sigma^0, \pi^+ \Sigma^-, \pi^- \Sigma^+, K^+ \Xi^-, K^0 \Xi^0$
		-1	-1	$K^- n, \pi^0 \Sigma^-, \pi^- \Sigma^0, \pi^- \Lambda, \eta \Sigma^-, K^0 \Xi^-$
		-2	-2	$\pi^- \Sigma^-$
1	0	$\frac{3}{2}$	2	$\pi^+ p, K^+ \Sigma^+$
		$\frac{1}{2}$	1	$\pi^0 p, \pi^+ n, \eta p, K^+ \Lambda, K^+ \Sigma^0, K^0 \Sigma^+$
		$-\frac{1}{2}$	0	$\pi^0 n, \pi^- p, \eta n, K^0 \Lambda, K^0 \Sigma^0, K^+ \Sigma^-$
		$-\frac{3}{2}$	-1	$\pi^- n, K^0 \Sigma^-$
2	1	1	2	$K^+ p$
		0	1	$K^+ n, K^0 p$
		-1	0	$K^0 n$

to order  $\mathcal{O}(m_q)$ . Therefore, the suitable choice of the channel dependent subtraction constants is essential. Investigation of their microscopic origin is an important work in future.

Generally speaking, the chiral unitary approach is one of the powerful phenomenological methods. It can reproduce cross sections and generate  $s$  wave resonances dynamically, once the subtraction constants are determined appropriately, using experimental data. However, it is not straightforward to apply the method to the channels where there are not sufficient experimental data, since they are required to determine the subtraction constants.

### Acknowledgements

We would like to thank Profs. E. Oset, H. -Ch. Kim and W. Weise for useful discussions.

Table IV. Table of  $D_i^{Z_1}$ .

meson	$\pi$	$K, \bar{K}$	$\eta$
$D_i^{Z_1}$	$2\hat{m}$	$\hat{m} + m_s$	$\frac{2}{3}(\hat{m} + 2m_s)$

## Appendix A

### — Coefficients of the $SU(3)$ breaking interaction —

Here we show the coefficients of the flavor  $SU(3)$  breaking terms in the meson-baryon interactions. The corresponding Lagrangian is given by

$$\begin{aligned} \mathcal{L}_{SB}^{(2)} = & \frac{Z_0}{4f^2} \text{Tr} \left( d_m \bar{B} \{ (2\Phi \mathbf{m} \Phi + \Phi^2 \mathbf{m} + \mathbf{m} \Phi^2), B \} + f_m \bar{B} [(2\Phi \mathbf{m} \Phi + \Phi^2 \mathbf{m} + \mathbf{m} \Phi^2), B] \right) \\ & + \frac{Z_1}{f^2} \text{Tr}(\bar{B} B) \text{Tr}(\mathbf{m} \Phi^2). \end{aligned} \quad (\text{A}\cdot 1)$$

From this Lagrangian, the basic interaction at the tree level is given by

$$\begin{aligned} V_{ij}^{(SB)} = & -\frac{1}{f^2} \left[ Z_0 \left( (A_{ij}^d d_m + A_{ij}^f f_m) \hat{m} + (B_{ij}^d d_m + B_{ij}^f f_m) m_s \right) \right. \\ & \left. + Z_1 \delta_{ij} D_i^{Z_1} \right] \sqrt{\frac{E_i + M_i}{2M_i}} \sqrt{\frac{E_j + M_j}{2M_j}}, \end{aligned} \quad (\text{A}\cdot 2)$$

where the coefficients  $A$ ,  $B$  and  $D$  are the numbers in matrix form and the indices  $(i, j)$  denote the channels of the meson-baryon scatterings as shown in Table III.

These channels are specified by two quantum numbers, the hypercharge  $Y$  and the third component of isospin  $I_3$ , or equivalently the strangeness  $S$  and the electric charge  $Q$ , through the Gell-Mann-Nakano-Nishijima relation<sup>64), 65)</sup>

$$Q = T_3 + \frac{Y}{2}, \quad S = Y - B, \quad (\text{A}\cdot 3)$$

where the baryon number  $B = 1$  for the meson-baryon scatterings.

The coefficient  $D_i^{Z_1}$  is specified only by the meson in channel  $i$  independently of baryons, because  $\text{Tr}(\bar{B} B)$  in the last term of Eq. (A·1) gives a common contribution to all baryons. Also, there is no off-diagonal component when the isospin symmetry is assumed. The explicit form of  $D_i^{Z_1}$  is shown in Table IV. The values of the coefficients  $A$  and  $B$  are shown in the following tables;

- Table VI ( $S = 1, Q = 1$ )
- Table VII ( $S = -3, Q = -1$ )
- Tables VIII and IX ( $S = 0, Q = 0$ )
- Tables X and XI ( $S = -2, Q = -1$ )
- Tables XII, XIII, XIV and XV ( $S = -1, Q = 0$ ).

From these tables, the coefficients  $A$  and  $B$  for all the channels can be derived, using symmetry relations.

First, the channels in the same  $S$  and different  $Q$  are related through the  $SU(2)$  Clebsch-Gordan coefficients due to the isospin symmetry. This is the relation among the channels in the block separated by the horizontal lines in table III.

Table V. Quantum numbers of channels  $i, j, i'$  and  $j'$ 

channel	hypercharge			third component of isospin		
	meson	baryon	total	meson	baryon	total
$i$	$y_i$	$Y - y_i$	$Y$	$i_{3i}$	$I_3 - i_{3i}$	$I_3$
$j$	$y_j$	$Y - y_j$	$Y$	$i_{3j}$	$I_3 - i_{3j}$	$I_3$
$i'$	$-y_i$	$-Y + y_i$	$-Y$	$-i_{3i}$	$-I_3 + i_{3i}$	$-I_3$
$j'$	$-y_j$	$-Y + y_j$	$-Y$	$-i_{3j}$	$-I_3 + i_{3j}$	$-I_3$

Table VI.  $A_{ij}^d, A_{ij}^f, B_{ij}^d$  and  $B_{ij}^f (S = 1, Q = 1)$ 

	$A_{ij}^d$		$A_{ij}^f$		$B_{ij}^d$		$B_{ij}^f$	
	$K^+ n$	$K^0 p$	$K^+ n$	$K^0 p$	$K^+ n$	$K^0 p$	$K^+ n$	$K^0 p$
$K^+ n$	$\frac{1}{2}$	$\frac{1}{2}$	$-\frac{1}{2}$	$\frac{1}{2}$	$\frac{1}{2}$	$\frac{1}{2}$	$-\frac{1}{2}$	$\frac{1}{2}$
$K^0 p$		$\frac{1}{2}$		$-\frac{1}{2}$		$\frac{1}{2}$		$-\frac{1}{2}$

Table VII.  $A_{ij}^d, A_{ij}^f, B_{ij}^d$  and  $B_{ij}^f (S = -3, Q = -1)$ 

	$A_{ij}^d$		$A_{ij}^f$		$B_{ij}^d$		$B_{ij}^f$	
	$K^- \Xi^0$	$K^0 \Xi^-$	$K^- \Xi^0$	$K^0 \Xi^-$	$K^- \Xi^0$	$K^0 \Xi^-$	$K^- \Xi^0$	$K^0 \Xi^-$
$K^0 \Xi^-$	$\frac{1}{2}$	$\frac{1}{2}$	$\frac{1}{2}$	$-\frac{1}{2}$	$\frac{1}{2}$	$\frac{1}{2}$	$\frac{1}{2}$	$-\frac{1}{2}$
$K^- \Xi^0$		$\frac{1}{2}$		$\frac{1}{2}$		$\frac{1}{2}$		$\frac{1}{2}$

Second, the coefficients of the sector  $(Y, I_3)$  are related with those of  $(-Y, -I_3)$ . Let us consider the channels  $(i, j)$  and  $(i', j')$  in the sectors  $(Y, I_3)$  and  $(-Y, -I_3)$ , respectively, as shown in Table V. Then the coefficients of the sector  $(-Y, -I_3)$  are given by

$$\begin{aligned}
 A_{i'j'}^d(-Y, -I_3) &= A_{ij}^d(Y, I_3), & A_{i'j'}^f(-Y, -I_3) &= -A_{ij}^f(Y, I_3), \\
 B_{i'j'}^d(-Y, -I_3) &= B_{ij}^d(Y, I_3), & B_{i'j'}^f(-Y, -I_3) &= -B_{ij}^f(Y, I_3).
 \end{aligned}
 \tag{A.4}$$

Comparing the Table VI ( $Y = 2, I_3 = 0$ ) and Table VII ( $Y = -2, I_3 = 0$ ), we find that the relation (A.4) is satisfied. Also, using the relation (A.4), the coefficients of the sector  $(S = -2, Q = 0)$  are obtained from the tables of the sector  $(S = 0, Q = 0)$ . For example, if we specify  $(i, j)$  to be  $(\pi^0 n, K^0 \Lambda)$ , the corresponding  $(i', j')$  is  $(\pi^0 \Xi^0, \bar{K}^0 \Lambda)$ . The coefficients for  $(i', j')$  are obtained by  $A_{i'j'}^d = \sqrt{3}/8$ ,  $A_{i'j'}^f = -3\sqrt{3}/8$ ,  $B_{i'j'}^d = 1/(8\sqrt{3})$  and  $B_{i'j'}^f = -\sqrt{3}/8$ . In this way we can derive all the coefficients which are not shown in the tables.

### References

- 1) N. Kaiser, P. B. Siegel, and W. Weise, Phys. Lett. **B362**, 23 (1995).
- 2) N. Kaiser, P. B. Siegel, and W. Weise, Nucl. Phys. **A594**, 325 (1995).
- 3) N. Kaiser, T. Waas, and W. Weise, Nucl. Phys. **A612**, 297 (1997).
- 4) B. Krippa, Phys. Rev. **C58**, 1333 (1998).
- 5) E. Oset and A. Ramos, Nucl. Phys. **A635**, 99 (1998).
- 6) M. F. M. Lutz and E. E. Kolomeitsev, Nucl. Phys. **A700**, 193 (2002).
- 7) S. Weinberg, Physica **A96**, 327 (1979); Nucl. Phys. **B363**, 3 (1991).
- 8) J. Gasser and H. Leutwyler, Ann. Phys. **158**, 142 (1984); Nucl. Phys. **B250**, 465 (1985); **B250**, 517 (1985); **B250**, 539 (1985).
- 9) E. Oset, A. Ramos, and C. Bennhold, Phys. Lett. **B527**, 99 (2002).

Table VIII.  $A_{ij}^d$  and  $A_{ij}^f$  ( $S = 0, Q = 0$ )

	$A_{ij}^d$						$A_{ij}^f$					
	$\pi^0 n$	$\pi^- p$	$\eta n$	$K^0 \Lambda$	$K^0 \Sigma^0$	$K^+ \Sigma^-$	$\pi^0 n$	$\pi^- p$	$\eta n$	$K^0 \Lambda$	$K^0 \Sigma^0$	$K^+ \Sigma^-$
$\pi^0 n$	1	0	$-\frac{1}{\sqrt{3}}$	$\frac{\sqrt{3}}{8}$	$\frac{3}{8}$	$\frac{3}{4\sqrt{2}}$	1	0	$-\frac{1}{\sqrt{3}}$	$\frac{3\sqrt{3}}{8}$	$-\frac{3}{8}$	$-\frac{3}{4\sqrt{2}}$
$\pi^- p$		1	$\sqrt{\frac{2}{3}}$	$-\frac{\sqrt{6}}{8}$	$\frac{3}{4\sqrt{2}}$	0		1	$\sqrt{\frac{2}{3}}$	$-\frac{3\sqrt{6}}{8}$	$-\frac{3}{4\sqrt{2}}$	0
$\eta n$			$\frac{1}{3}$	$-\frac{1}{24}$	$-\frac{1}{8\sqrt{3}}$	$\frac{1}{4\sqrt{6}}$			$\frac{1}{3}$	$-\frac{1}{8}$	$\frac{1}{8\sqrt{3}}$	$-\frac{1}{4\sqrt{6}}$
$K^0 \Lambda$				$\frac{5}{6}$	$-\frac{1}{2\sqrt{3}}$	$\frac{1}{\sqrt{6}}$				0	0	0
$K^0 \Sigma^0$					$\frac{1}{2}$	0					0	$\frac{1}{\sqrt{2}}$
$K^+ \Sigma^-$						$\frac{1}{2}$						$-\frac{1}{2}$

Table IX.  $B_{ij}^d$  and  $B_{ij}^f$  ( $S = 0, Q = 0$ )

	$B_{ij}^d$						$B_{ij}^f$					
	$\pi^0 n$	$\pi^- p$	$\eta n$	$K^0 \Lambda$	$K^0 \Sigma^0$	$K^+ \Sigma^-$	$\pi^0 n$	$\pi^- p$	$\eta n$	$K^0 \Lambda$	$K^0 \Sigma^0$	$K^+ \Sigma^-$
$\pi^0 n$	0	0	0	$\frac{1}{8\sqrt{3}}$	$\frac{1}{8}$	$\frac{1}{4\sqrt{2}}$	0	0	0	$\frac{\sqrt{3}}{8}$	$-\frac{1}{8}$	$-\frac{1}{4\sqrt{2}}$
$\pi^- p$		0	0	$-\frac{1}{4\sqrt{6}}$	$\frac{1}{4\sqrt{2}}$	0		0	0	$-\frac{\sqrt{6}}{8}$	$-\frac{1}{4\sqrt{2}}$	0
$\eta n$			$\frac{4}{3}$	$\frac{5}{24}$	$\frac{5}{8\sqrt{3}}$	$-\frac{5}{4\sqrt{6}}$			$-\frac{4}{3}$	$\frac{5}{8}$	$-\frac{5}{8\sqrt{3}}$	$\frac{5}{4\sqrt{6}}$
$K^0 \Lambda$				$\frac{5}{6}$	$-\frac{1}{2\sqrt{3}}$	$\frac{1}{\sqrt{6}}$				0	0	0
$K^0 \Sigma^0$					$\frac{1}{2}$	0					0	$\frac{1}{\sqrt{2}}$
$K^+ \Sigma^-$						$\frac{1}{2}$						$-\frac{1}{2}$

Table X.  $A_{ij}^d$  and  $A_{ij}^f$  ( $S = -2, Q = -1$ )

	$A_{ij}^d$						$A_{ij}^f$					
	$\pi^0 \Xi^-$	$\pi^- \Xi^0$	$\eta \Xi^-$	$K^- \Lambda$	$K^- \Sigma^0$	$\bar{K}^0 \Sigma^-$	$\pi^0 \Xi^-$	$\pi^- \Xi^0$	$\eta \Xi^-$	$K^- \Lambda$	$K^- \Sigma^0$	$\bar{K}^0 \Sigma^-$
$\pi^0 \Xi^-$	1	0	$\frac{1}{\sqrt{3}}$	$-\frac{\sqrt{3}}{8}$	$\frac{3}{8}$	$-\frac{3}{4\sqrt{2}}$	-1	0	$-\frac{1}{\sqrt{3}}$	$\frac{3\sqrt{3}}{8}$	$\frac{3}{8}$	$-\frac{3}{4\sqrt{2}}$
$\pi^- \Xi^0$		1	$\sqrt{\frac{2}{3}}$	$-\frac{\sqrt{6}}{8}$	$-\frac{3}{4\sqrt{2}}$	0		-1	$-\sqrt{\frac{2}{3}}$	$\frac{3\sqrt{6}}{8}$	$-\frac{3}{4\sqrt{2}}$	0
$\eta \Xi^-$			$\frac{1}{3}$	$-\frac{1}{24}$	$\frac{1}{8\sqrt{3}}$	$\frac{1}{4\sqrt{6}}$			$-\frac{1}{3}$	$\frac{1}{8}$	$\frac{1}{8\sqrt{3}}$	$\frac{1}{4\sqrt{6}}$
$K^- \Lambda$				$\frac{5}{6}$	$\frac{1}{2\sqrt{3}}$	$\frac{1}{\sqrt{6}}$				0	0	0
$K^- \Sigma^0$					$\frac{1}{2}$	0					0	$\frac{1}{\sqrt{2}}$
$\bar{K}^0 \Sigma^-$						$\frac{1}{2}$						$-\frac{1}{2}$

Table XI.  $B_{ij}^d$  and  $B_{ij}^f$  ( $S = -2, Q = -1$ )

	$B_{ij}^d$						$B_{ij}^f$					
	$\pi^0 \Xi^-$	$\pi^- \Xi^0$	$\eta \Xi^-$	$K^- \Lambda$	$K^- \Sigma^0$	$\bar{K}^0 \Sigma^-$	$\pi^0 \Xi^-$	$\pi^- \Xi^0$	$\eta \Xi^-$	$K^- \Lambda$	$K^- \Sigma^0$	$\bar{K}^0 \Sigma^-$
$\pi^0 \Xi^-$	0	0	0	$-\frac{1}{8\sqrt{3}}$	$\frac{1}{8}$	$-\frac{1}{4\sqrt{2}}$	0	0	0	$\frac{\sqrt{3}}{8}$	$\frac{1}{8}$	$-\frac{1}{4\sqrt{2}}$
$\pi^- \Xi^0$		0	0	$-\frac{1}{4\sqrt{6}}$	$-\frac{1}{4\sqrt{2}}$	0		0	0	$\frac{3}{4\sqrt{6}}$	$-\frac{1}{4\sqrt{2}}$	0
$\eta \Xi^-$			$\frac{4}{3}$	$\frac{5}{24}$	$-\frac{5}{8\sqrt{3}}$	$-\frac{5}{4\sqrt{6}}$			$\frac{4}{3}$	$-\frac{5}{8}$	$-\frac{5}{8\sqrt{3}}$	$-\frac{5}{4\sqrt{6}}$
$K^- \Lambda$				$\frac{5}{6}$	$\frac{1}{2\sqrt{3}}$	$\frac{1}{\sqrt{6}}$				0	0	0
$K^- \Sigma^0$					$\frac{1}{2}$	0					0	$\frac{1}{\sqrt{2}}$
$\bar{K}^0 \Sigma^-$						$\frac{1}{2}$						$-\frac{1}{2}$

- 10) T. Inoue, E. Oset, and M. J. Vicente Vacas, Phys. Rev. **C65**, 035204 (2002).
- 11) A. Ramos, E. Oset, and C. Bennhold, nucl-th/0204044.
- 12) J. A. Oller and U. G. Meissner, Phys. Lett. **B500**, 263 (2001).
- 13) D. Jido, E. Oset, and A. Ramos, Phys. Rev. **C66**, 055203 (2002).
- 14) D. Jido, J. A. Oller, E. Oset, A. Ramos, and U. G. Meissner, nucl-th/0303062.
- 15) T. Hyodo, S. I. Nam, D. Jido, and A. Hosaka, nucl-th/0212026.

Table XII.  $A_{ij}^d(S = -1, Q = 0)$ 

	$K^-p$	$\bar{K}^0n$	$\pi^0\Lambda$	$\pi^0\Sigma^0$	$\eta\Lambda$	$\eta\Sigma^0$	$\pi^+\Sigma^-$	$\pi^-\Sigma^+$	$K^+\Xi^-$	$K^0\Xi^0$
$K^-p$	1	$\frac{1}{2}$	$-\frac{\sqrt{3}}{8}$	$\frac{3}{8}$	$-\frac{1}{24}$	$\frac{1}{8\sqrt{3}}$	0	$\frac{3}{4}$	0	0
$\bar{K}^0n$		1	$\frac{\sqrt{3}}{8}$	$\frac{3}{8}$	$-\frac{1}{24}$	$-\frac{1}{8\sqrt{3}}$	$\frac{3}{4}$	0	0	0
$\pi^0\Lambda$			$\frac{2}{3}$	0	0	$\frac{2}{3}$	0	0	$-\frac{\sqrt{3}}{8}$	$\frac{\sqrt{3}}{8}$
$\pi^0\Sigma^0$				2	$\frac{2}{3}$	0	0	0	$\frac{3}{8}$	$\frac{3}{8}$
$\eta\Lambda$					$\frac{2}{9}$	0	$\frac{2}{3}$	$\frac{2}{3}$	$-\frac{1}{24}$	$-\frac{1}{24}$
$\eta\Sigma^0$						$\frac{2}{3}$	0	0	$\frac{1}{8\sqrt{3}}$	$-\frac{1}{8\sqrt{3}}$
$\pi^+\Sigma^-$							2	0	$\frac{3}{4}$	0
$\pi^-\Sigma^+$								2	0	$\frac{3}{4}$
$K^+\Xi^-$									1	$\frac{1}{2}$
$K^0\Xi^0$										1

Table XIII.  $A_{ij}^f(S = -1, Q = 0)$ 

	$K^-p$	$\bar{K}^0n$	$\pi^0\Lambda$	$\pi^0\Sigma^0$	$\eta\Lambda$	$\eta\Sigma^0$	$\pi^+\Sigma^-$	$\pi^-\Sigma^+$	$K^+\Xi^-$	$K^0\Xi^0$
$K^-p$	0	$\frac{1}{2}$	$-\frac{3\sqrt{3}}{8}$	$-\frac{3}{8}$	$-\frac{1}{8}$	$-\frac{1}{8\sqrt{3}}$	0	$-\frac{3}{4}$	0	0
$\bar{K}^0n$		0	$\frac{3\sqrt{3}}{8}$	$-\frac{3}{8}$	$-\frac{1}{8}$	$\frac{1}{8\sqrt{3}}$	$-\frac{3}{4}$	0	0	0
$\pi^0\Lambda$			0	0	0	0	0	0	$\frac{3\sqrt{3}}{8}$	$-\frac{3\sqrt{3}}{8}$
$\pi^0\Sigma^0$				0	0	0	0	0	$\frac{3}{8}$	$\frac{3}{8}$
$\eta\Lambda$					0	0	0	0	$\frac{1}{8}$	$\frac{1}{8}$
$\eta\Sigma^0$						0	$\frac{2}{\sqrt{3}}$	$-\frac{2}{\sqrt{3}}$	$\frac{1}{8\sqrt{3}}$	$-\frac{1}{8\sqrt{3}}$
$\pi^+\Sigma^-$							0	0	$\frac{3}{4}$	0
$\pi^-\Sigma^+$								0	0	$\frac{3}{4}$
$K^+\Xi^-$									0	$-\frac{1}{2}$
$K^0\Xi^0$										0

- 16) A. Gomez Nicola, J. Nieves, J. R. Pelaez, and E. Ruiz Arriola, Phys. Lett. **B486**, 77 (2000).
- 17) G. F. Chew and S. Mandelstam, Phys. Rev. **119**, 467 (1960).
- 18) U.-G. Meissner and J. A. Oller, Nucl. Phys. **A673**, 311 (2000).
- 19) For example, J. F. Donoghue, E. Golowich, and B. R. Holstein, *Dynamics of the standard model* (Cambridge University Press, London, 1992).
- 20) R. J. Nowak *et al.*, Nucl. Phys. **B139**, 61 (1978).
- 21) D. N. Tovee *et al.*, Nucl. Phys. **B33**, 493 (1971).
- 22) T. S. Mast, M. Alston-Garnjost, R. O. Bangerter, A. S. Barbaro-Galtieri, F. T. Solmitz, and R. D. Tripp, Phys. Rev. **D14**, 13 (1976).
- 23) J. Ciborowski *et al.*, J. Phys. **G8**, 13 (1982).
- 24) R. O. Bangerter, M. Alston-Garnjost, A. S. Barbaro-Galtieri, T. S. Mast, F. T. Solmitz, and R. D. Tripp, Phys. Rev. **D23**, 1484 (1981).
- 25) T. S. Mast, M. Alston-Garnjost, R. O. Bangerter, A. S. Barbaro-Galtieri, F. T. Solmitz, and R. D. Tripp, Phys. Rev. **D11**, 3078 (1975).
- 26) M. Sakitt, T. B. Day, R. G. Glasser, N. Seeman, J. H. Friedman, W. E. Humphrey, and R. R. Ross, Phys. Rev. **139**, B719 (1965).
- 27) M. B. Watson, M. Ferro-Luzzi, and R. D. Tripp, Phys. Rev. **131**, 2248 (1963).
- 28) M. Ferro-Luzzi, R. D. Tripp, and M. B. Watson, Phys. Rev. Lett. **8**, 28 (1962).
- 29) M. Csejthey-Barth *et al.*, Phys. Lett. **16**, 89 (1965).
- 30) P. Nordin, Jr., Phys. Rev. **123**, 2168 (1961).
- 31) W. Kittel, G. Ptter, and I. Wacek, Phys. Lett. **21**, 349 (1966).
- 32) H. Göing, Nuovo Cim. **16**, 848 (1960).
- 33) J. K. Kim, Phys. Rev. Lett. **14**, 29 (1965); Columbia University Report, Nevis 149 (1966).
- 34) G. P. Gopal, R. T. Ross, A. J. Van Horn, A. C. McPherson, E. F. Clayton, T. C. Bacon, and I. Butterworth, Nucl. Phys. **B119**, 362 (1977).

Table XIV.  $B_{ij}^d(S = -1, Q = 0)$ 

	$K^-p$	$\bar{K}^0n$	$\pi^0\Lambda$	$\pi^0\Sigma^0$	$\eta\Lambda$	$\eta\Sigma^0$	$\pi^+\Sigma^-$	$\pi^-\Sigma^+$	$K^+\Xi^-$	$K^0\Xi^0$
$K^-p$	1	$\frac{1}{2}$	$-\frac{1}{8\sqrt{3}}$	$\frac{1}{8}$	$\frac{5}{24}$	$-\frac{5}{8\sqrt{3}}$	0	$\frac{1}{4}$	0	0
$\bar{K}^0n$		1	$\frac{1}{8\sqrt{3}}$	$\frac{1}{8}$	$\frac{5}{24}$	$\frac{5}{8\sqrt{3}}$	$\frac{1}{4}$	0	0	0
$\pi^0\Lambda$			0	0	0	0	0	0	$-\frac{1}{8\sqrt{3}}$	$\frac{1}{8\sqrt{3}}$
$\pi^0\Sigma^0$				0	0	0	0	0	$\frac{1}{8}$	$\frac{1}{8}$
$\eta\Lambda$					$\frac{16}{9}$	0	0	0	$\frac{5}{24}$	$\frac{5}{24}$
$\eta\Sigma^0$						0	0	0	$-\frac{5}{8\sqrt{3}}$	$\frac{5}{8\sqrt{3}}$
$\pi^+\Sigma^-$							0	0	$\frac{1}{4}$	0
$\pi^-\Sigma^+$								0	0	$\frac{1}{4}$
$K^+\Xi^-$									1	$\frac{1}{2}$
$K^0\Xi^0$										1

Table XV.  $B_{ij}^f(S = -1, Q = 0)$ 

	$K^-p$	$\bar{K}^0n$	$\pi^0\Lambda$	$\pi^0\Sigma^0$	$\eta\Lambda$	$\eta\Sigma^0$	$\pi^+\Sigma^-$	$\pi^-\Sigma^+$	$K^+\Xi^-$	$K^0\Xi^0$
$K^-p$	0	$\frac{1}{2}$	$-\frac{\sqrt{3}}{8}$	$-\frac{1}{8}$	$\frac{5}{8}$	$\frac{5}{8\sqrt{3}}$	0	$-\frac{1}{4}$	0	0
$\bar{K}^0n$		0	$\frac{\sqrt{3}}{8}$	$-\frac{1}{8}$	$\frac{5}{8}$	$-\frac{5}{8\sqrt{3}}$	$-\frac{1}{4}$	0	0	0
$\pi^0\Lambda$			0	0	0	0	0	0	$\frac{\sqrt{3}}{8}$	$-\frac{\sqrt{3}}{8}$
$\pi^0\Sigma^0$				0	0	0	0	0	$\frac{1}{8}$	$\frac{1}{8}$
$\eta\Lambda$					0	0	0	0	$-\frac{5}{8}$	$-\frac{5}{8}$
$\eta\Sigma^0$						0	0	0	$-\frac{5}{8\sqrt{3}}$	$\frac{5}{8\sqrt{3}}$
$\pi^+\Sigma^-$							0	0	$\frac{1}{4}$	0
$\pi^-\Sigma^+$								0	0	$\frac{1}{4}$
$K^+\Xi^-$									0	$-\frac{1}{2}$
$K^0\Xi^0$										0

- 35) R. J. Hemingway, Nucl. Phys. **B253**, 742 (1985).
- 36) M. Batinic, I. Slaus, A. Svarc, and B. M. K. Nefkens, Phys. Rev. **C51**, 2310 (1995).
- 37) J. C. Hart *et al.*, Nucl. Phys. **B166**, 73 (1980).
- 38) D. H. Saxon *et al.*, Nucl. Phys. **B162**, 522 (1980).
- 39) R. D. Baker *et al.*, Nucl. Phys. **B145**, 402 (1978).
- 40) R. D. Baker *et al.*, Nucl. Phys. **B141**, 29 (1978).
- 41) B. Nelson *et al.*, Phys. Rev. Lett. **31**, 901 (1973).
- 42) D. W. Thomas, A. Engler, H. E. Fisk, and R. W. Kraemer, Nucl. Phys. **B56**, 15 (1973).
- 43) J. J. Jones, T. Bowen, W. R. Dawes, D. A. Delise, E. W. Jenkins, R. M. Kalbach, E. I. Malamud, K. J. Nield, and D. V. Petersen, Phys. Rev. Lett. **26**, 860 (1971).
- 44) T. O. Binford, M. L. Good, V. G. Lind, D. Stern, R. Krauss, and E. Dettman Phys. Rev. **183**, 1134 (1969).
- 45) O. Van Dyck, R. Blumenthal, S. Frankel, V. Highland, J. Nagy, T. Sloan, M. Takats, W. Wales, and R. Werbeck, Phys. Rev. Lett. **23**, 50 (1969).
- 46) T. M. Knasel *et al.*, Phys. Rev. **D11**, 1 (1975).
- 47) R. L. Crollius, V. Cook, B. Cork, D. Keefe, L. T. Kerth, W. M. Layson, and W. A. Wenzel, Phys. Rev. **155**, 1455 (1967).
- 48) J. Keren, Phys. Rev. **133**, B457 (1963).
- 49) L. L. Yoder, C. T. Coffin, D. I. Meyer, and K. M. Terwilliger, Phys. Rev. **132**, 1778 (1963).
- 50) L. B. Leipuner and R. K. Adair, Phys. Rev. **109**, 1358 (1958).
- 51) L. Bertanza, P. L. Connolly, B. B. Culwick, F. R. Eisler, T. Morris, R. Palmer, A. Prodell, and N. P. Samios, Phys. Rev. Lett. **8**, 332 (1962).
- 52) F. S. Crawford, R. L. Douglass, M. L. Good, G. R. Kalbfleisch, M. L. Stevenson, and H. K. Ticho, Phys. Rev. Lett. **3**, 394 (1959).
- 53) R. T. V. de Walle, C. L. A. Pols, D. J. Schotanus, H. J. G. M. Tiecke, and D. Z. Toet, Nuovo Cim. **A53**, 745 (1968).

- 54) O. Goussu, M. Sene, B. Ghidini, S. Mongelli, A. Romano, P. Waloschek, V. Alles-Borelli, Nuovo Cim. **42A**, 606 (1966).
- 55) F. Eisler *et al.*, Nuovo Cim. **10**, 468 (1958).
- 56) Center of Nuclear Study, <http://gwdac.phys.gwu.edu> .
- 57) M. Gell-Mann, R. J. Oakes, and B. Renner, Phys. Rev. **175**, 2195 (1968).
- 58) M. Gell-Mann, Phys. Rev. **125**, 1067 (1962).
- 59) S. Okubo, Prog. Theor. Phys. **27**, 949 (1962).
- 60) P. J. Fink, G. He, R. H. Landau and J. W. Schnick, Phys. Rev. C **41**, 2720 (1990).
- 61) D. Jido, A. Hosaka, J. C. Nacher, E. Oset, and A. Ramos, Phys. Rev. **C66**, 025203 (2002).
- 62) C. Garcia-Recio, J. Nieves, E. Ruiz Arriola, and M. J. Vicente Vacas, hep-ph/0210311.
- 63) C. Bennhold and H. Tanabe, Nucl. Phys. **A530**, 625 (1991).
- 64) M. Gell-Mann, Phys. Rev. **92**, 833 (1954).
- 65) T. Nakano and K. Nishijima, Prog. Theor. Phys. **10**, 581 (1954).